

See discussions, stats, and author profiles for this publication at: <https://www.researchgate.net/publication/244507566>

# Spectroscopy and photophysics of styrylquinoline-type HIV1 integrase inhibitors and its oxidized forms studied by steady state and time resolved absorption and fluorescence

ARTICLE *in* PHYSICAL CHEMISTRY CHEMICAL PHYSICS · JANUARY 2001

Impact Factor: 4.49 · DOI: 10.1039/b102555b

CITATIONS

9

READS

6

12 AUTHORS, INCLUDING:



**Didier Desmaële**

Université Paris-Sud 11

197 PUBLICATIONS 4,352 CITATIONS

SEE PROFILE



**Patrick Tauc**

Ecole normale supérieure de Cachan

75 PUBLICATIONS 1,776 CITATIONS

SEE PROFILE



**Pascal Pernot**

French National Centre for Scientific Resea...

140 PUBLICATIONS 1,218 CITATIONS

SEE PROFILE



**Mironel Enescu**

University of Franche-Comté

49 PUBLICATIONS 476 CITATIONS

SEE PROFILE

# Spectroscopy and photophysics of styrylquinoline-type HIV-1 integrase inhibitors and its oxidized forms studied by steady state and time resolved absorption and fluorescence

Rolande Burdujan,<sup>a</sup> Jean d'Angelo,<sup>b</sup> Didier Desmaële,<sup>b</sup> Fatima Zouhiri,<sup>b</sup> Patrick Tauc,<sup>c</sup> Jean-Claude Brochon,<sup>c</sup> Christian Auclair,<sup>d</sup> Jean-François Mouscadet,<sup>d</sup> Pascal Pernot,<sup>e</sup> Francis Tfibel,<sup>a</sup> Mironel Enescu<sup>a</sup> and Marie-Pierre Fontaine-Aupart<sup>\*a</sup>

<sup>a</sup> Laboratoire de Photophysique Moléculaire, UPR 3361 CNRS, Université Paris-Sud, 91405 Orsay Cedex, France. E-mail: marie-pierre.fontaine-aupart@ppm.u-psud.fr

<sup>b</sup> Centre d'Etudes Pharmaceutique, Laboratoire de Chimie Organique, UPRES-A 8076 CNRS, Université Paris-Sud, 92296 Chatenay Malabry, France

<sup>c</sup> Laboratoire de Biotechnologies et de Pharmacologie Génétique Appliquée, UMR 8532, ENS Cachan, 92435 Cachan, France

<sup>d</sup> Physicochimie et Pharmacologie des Macromolécules Biologiques, UMR 8532 CNRS, Institut Gustave Roussy, Villejuif, France

<sup>e</sup> Laboratoire de Chimie Physique, Université Paris-Sud, 91405 Orsay Cedex, France

Received 19th March 2001, Accepted 10th July 2001

First published as an Advance Article on the web 7th August 2001

The geometric and electronic structure in solution of a new 2-styrylquinoline-type inhibitor of the HIV1-integrase was examined for the first time by following changes in the photophysical properties of the chromophore using steady state as well as time resolved absorption and fluorescence methods. The results obtained under different conditions of pH and solvent revealed that there are at least two rotamers in the ground state which exhibit different photophysical and photochemical properties. Picosecond fluorescence and absorption measurements gave evidence for a very short ( $\sim 20$ – $30$  ps) singlet excited state lifetime for one conformer and a much longer one for the other conformer, from a few hundreds of picoseconds up to nanoseconds, depending on the solvent characteristics. At physiological pH, the longer lived conformer can also undergo oxygen oxidation or photooxidation giving rise to the formation of the semiquinone radical and ultimately to a stable orthoquinone species. The role played by the singlet excited state of the rotamer on the photooxidation process is also detailed using picosecond and nanosecond absorption measurements.

## Introduction

The replicative life cycle of the HIV virus requires the integration of viral DNA into genomic DNA of the host cell, a process which is mediated by the viral protein integrase (IN). The development of inhibitors of IN activity constitutes a new challenge for the treatment of HIV-1 infection.<sup>1</sup> Several inhibitors of HIV-1 integrase have been now identified, but only a few display antiviral activity in cells. A promising class of such antiviral agents based on a 2-styrylquinoline-like structure (Scheme 1) has attracted widespread interest since these molecules inhibit HIV integrase function both *in vitro* and *in vivo* and are devoid of cellular toxicity.<sup>2–4</sup>

No contribution has appeared up to now about the physico-chemical properties of compound **1** and its analogs (Scheme 1) which would allow an understanding of the biological function of these molecules at the molecular level, including the nature of the interactions with the biological targets. Since compound **1** is a *trans*-2-styrylquinoline-like chromophore, different conformational geometries (tautomers and rotamers) of the drug should exist in solution.<sup>5–7</sup> Thus, the physico-chemical as well as the photochemical behavior of **1** are the results of the different contributions of these individual conformers<sup>5–10</sup> and it is of importance to know which is the predominant form of the drug in the various environ-

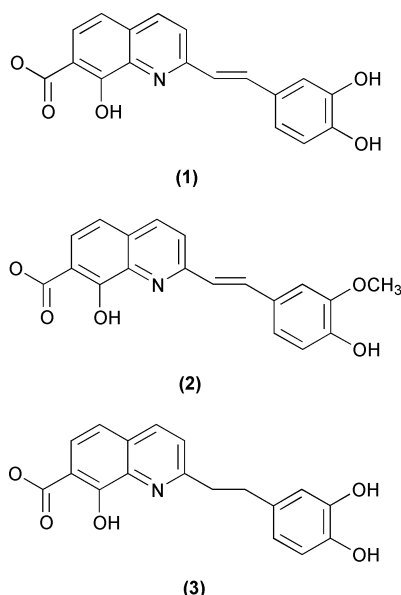
mental conditions and in its biological binding site. For this purpose, we have carried out a detailed study of the steady state and time resolved absorption and fluorescence properties of **1**. The spectroscopic properties of the drug in various solvents and in aqueous solutions at various pH values were studied with the aim to obtain information on the influence of the environmental conditions on its stability, its geometric and electronic structure in solution. Absorption and emission spectra, fluorescence decays and quantum yields have been interpreted in terms of the existence of an equilibrium between at least two rotamers depending on the protonation state of the drug and the protic or aprotic character of the solvent.

Furthermore, we have also proved the ability of **1** to be oxidized by oxygen or as a result of photonic excitation and characterized the intermediates involved in such a process by subpicosecond and nanosecond laser flash photolysis. The picosecond formation of a semiquinone radical was demonstrated and a mechanism for the formation of the more stable orthoquinone species was proposed.

## Materials and methods

### Samples

The compound **1** and the analogs **2** and **3** were prepared in the Laboratoire de Chimie Organique (Chatenay Malabry), as



**Scheme 1** Structure of **1** and analogs **2** and **3**

described in the literature.<sup>2</sup> The drugs were first dissolved ( $10^{-1}$  M) in DMSO solution (Prolabo, Normapur) and then diluted in buffers prepared from deionized water (passed through an ion exchange column, Bioblock Scientific type U3) twice distilled in an all-quartz two stage Heraeus set-up. The final percentage of DMSO never exceeded 2%. All the solvents were of spectroscopy grade from Merck. The percentage of water in ethanol was 5%. For the pH influence study, compound **1** was diluted in HCl at pH 2.0, in 20 mM Tris-HCl or 20 mM phosphate buffer ( $\text{KH}_2\text{PO}_4/\text{K}_2\text{HPO}_4$ ) for pH ranging from 7.0 to 8.5 and in 20 mM glycine buffer for pH > 8.5. Some results were obtained in 50 mM borate buffer at pH 8.0. Salts used were of analytical grade (Merck).

The samples were deaerated by bubbling argon through the solution prior to the experiments. The oxygenated samples were obtained by maintaining 1 atm  $\text{O}_2$  upon the solution. All the gases were from Alphagaz with a purity of 99.99%. All the measurements were carried out at room temperature (298 K).

### Steady state experiments

The absorption and fluorescence steady state spectra were measured respectively with a Cary 210 (Varian) spectrophotometer and a Perkin-Elmer MPF3L fluorimeter. The spectra were recorded with home-made computer-controlled acquisition systems. In fluorescence experiments, the absorbance was usually less than 0.1 at the excitation wavelength. Excitation spectra were corrected for the fluctuations of the Xe-lamp intensity in the range 270–380 nm. Under these conditions, the spectral resolution of the fluorescence excitation spectra was the same as that of the absorption spectra.

The concentration of each compound was determined by weighing and used to estimate the molar absorption coefficient of the chromophore. The fluorescence quantum yield determination was carried out using 9,10-diphenylanthracene (DPA) in cyclohexane as a reference ( $\lambda_{\text{exc}} = 366$  nm;  $\Phi_f = 1$  under deaerated conditions)<sup>11</sup> according to the following relationship:

$$\phi_{\text{fx}} = \phi_{\text{fs}}(F_{\text{s}} A_{\text{x}}/F_{\text{x}} A_{\text{s}})(n_{\text{s}}^2/n_{\text{x}}^2)$$

where the subscript x refers to the unknown and the subscript s to the standard,  $A$  is the absorbance at the excitation wavelength,  $F$  is the integrated emission across the band and  $n$  the refractive index of the solvent.

### Time resolved fluorescence set-up

Fluorescence decays were measured by the time-correlated single photon counting technique.<sup>12,13</sup> The excitation light

pulse source was a Ti-sapphire subpicosecond laser (Tsunami, Spectra Physics) associated with a third harmonic generator tuned at 320 nm and was vertically polarized. The repetition of the laser was set down to 4 MHz and the pulse duration was 1 ps. Fluorescence emission was detected through a monochromator (Jobin-Yvon H10) set at 460 nm for dioxane experiments and at 540 nm for the other conditions ( $\Delta\lambda = 16$  nm), by a microchannel plate photomultiplier (Hamamatsu R1564U-06) connected to an amplifier, Phillips Scientific 6954 (gain 50). The excitation light pulse was triggered by a Hamamatsu photodiode (S4753). The pulse signal was amplified, shaped and connected to the stop input of the TAC (Time Amplitude Converter, Ortec 457) through a discriminator (Tenelec 453). The function of the instrumental response (100 ps) was recorded by detecting the light scattered by a water solution. The time scaling was 8.14 ps or 34.6 ps per channel and 2048 channels were used. Total fluorescence intensity,  $i(t)$ , was recorded by orientating the emission polarizer at the “magic” angle of  $54.75^\circ$ . The fluorescence decay and the instrumental response profile were collected alternately during 90 s and 30 s, respectively, over at least 20 periods until the total count for the fluorescence decay reached 12–16 millions (giving approximately  $10^5$  counts in the peak channel). To reduce the pileup errors from the time-amplitude converter, the counting rate never exceeded 10 kHz. The microcell (volume 50  $\mu\text{l}$ ) was thermostated with a Haake type-F3 circulating bath.

Analysis of fluorescence decay  $i(t)$  was performed by the quantified maximum entropy method (MEM).<sup>14,15</sup> Time resolved fluorescence decay data were fitted to a function that is a sum of 100 discrete exponentials. The explored lifetime domain ranges from 0.02 to 5 ns in a logarithm scale. The recovered distribution shows rather narrow peaks (data not shown), the positions of which are summarized in Table 1. The time resolution obtained after pulse convolution is  $\sim 20$  ps.

### Time-resolved absorption experiments

Subpicosecond laser photolysis was performed by a pump-probe method described previously.<sup>16</sup> Briefly, the laser system was the second harmonic of a Nd:YAG-pumped dye laser which delivers 0.5 ps pulses at a repetition rate of 10 Hz. The laser was used at 630 nm and frequency doubled to provide 15  $\mu\text{J}$  excitation pulses at 315 nm. The non-converted fraction of the laser beam ( $\lambda = 630$  nm) was focussed into water to generate a white light continuum used as a probing beam. The two probing beams, sample and reference, were simultaneously analyzed with a polychromator (Jarrell-Ash, entrance slit 100  $\mu\text{m}$ ) and an OMA Spec 4000 System (EG&G, Princeton Applied Research) equipped with a CCD detector. The time resolution of the system was less than 1 ps. The polarization of the pump light was set at the magic angle ( $54.7^\circ$ ) relative to the polarization of the probe light. In a given experiment, transient spectra were determined for a set-up of 20 chosen delay times of the probing beam with respect to the pumping beam (from  $-4$  ps to  $+400$  ps) which were automatically scanned at least 30 times. For each delay, the data were accumulated over 50 laser shots every scan. All of the wavelengths do not arrive at the sample at the same time owing to dispersion effects (group velocity and continuum generation), thus the transient spectra were corrected for this wavelength dependence of the delay times.

The excitation source of the nanosecond photolysis system was a Nd:YAG laser (Quantel, YG 441) of 3 ns full-width at half-maximum with third harmonic (355 nm) generation. The 355 nm beam was directed onto one side of a 10 mm square silica cell containing the sample. The transient transmission variations were monitored at right angles to the excitation in a cross beam arrangement using a xenon flash lamp, a mono-

**Table 1** Singlet excited state decay parameters and fluorescence quantum yields of compound **1** in different solvents and at different pH. The excitation wavelength is 320 nm and the drug concentration 15  $\mu\text{M}$

	$\tau_1/\text{ps}$ ( $\pm 15\%$ )	$A_1$ ( $\pm 2\%$ )	$\tau_2/\text{ps}$ ( $\pm 10\%$ )	$A_2$ ( $\pm 2\%$ )	$\tau_3/\text{ns}$ ( $\pm 10\%$ )	$A_3$ ( $\pm 2\%$ )	$\chi^2$	$\phi_f$ ( $\pm 0.01$ )
HCl pH 2.0	20	100					1.5	
Tris-HCl pH 7.0	30	30	230	70			1.75	0.02
Tris-HCl pH 8.0	30	40	220	60			1.8	0.02
Borate pH 8.0	20	100					2.5	
Dioxane			910	52	1.6	48	1.44	0.11
DMSO	50	7	650	31	3.0	62	1.47	0.14
Ethanol (5 % water)	50	45	290 <sup>a</sup> 780	12 31	1.7	12	1.3	0.04

<sup>a</sup> This component is due to the of 5% of water in the ethanol used.

chromator, a photomultiplier (HTV R928, response time 1 ns) and a digitized oscilloscope (Tektronix 2440) controlled by a microcomputer. The fluence of the incident laser pulse in the sample was obtained by calibration of the joulemeter using anthracene in deaerated cyclohexane as a triplet actinometer.<sup>17</sup>

The transient absorption data can be expressed as a sum of contributions from the spectrally active species:

$$\Delta A(\lambda, t) = \sum_i E_i(\lambda) D_i(t)$$

where  $E_i(\lambda)$  is the absorption spectrum of species  $i$ , and  $D_i(t)$  the corresponding kinetic evolution functions. Then, a kinetic scheme, using a compartmental-global analysis method, is designed where kinetic parameters and absorption spectra are simultaneously recovered.<sup>18</sup> The kinetic parameters are determined by non-linear iterative convolution method minimizing the sum of weighted-least-squares,<sup>18</sup> whereas the absorption spectra are calculated for each set of kinetic parameters by a least-squares algorithm.<sup>18</sup> In the absence of a normalization reference, no attempt is made to determine the spectral weights for each species.

### Drug irradiations

Steady state photolysis of drug **1** in Tris buffer solution (pH 7) was performed by irradiating the samples with an OSRAM-75W1 xenon lamp whose output was passed through a filter (Schott WG 345) to select wavelengths higher than 315 nm. The photochemical effects on the drug were also induced by exciting **1** with nanosecond laser pulses using the flash photolysis set-up (*vide supra*). These laser experiments allowed us to check the monophotonic character of the photoinduced effects.

## Results and discussion

### Spectral evidence for the existence of rotamers in the ground state

Compound **1** is a *trans*-2-styrylquinoline-like molecule and thus likely to exist as different conformational isomers involving rotation around the quasi-single bond between the styryl and quinoline moieties.<sup>5–7</sup> Detailed information on the existence of such ground state rotamers can be obtained from their absorption, excitation and emission spectra as well as the kinetic parameters of excited state deactivation.

The absorption spectra of compound **1** at pH 7.0 is illustrated in Fig. 1. Two distinct electronic transitions are observed, the highest one centered at 330 nm with a shoulder at 355 nm and a minor absorption band at 260 nm. The similarity between the absorption spectra of **1** and of styrylquinolines<sup>7,8</sup> allows a phenomenological attribution of the absorption bands to the different parts of the molecule.

The transition centered at 260 nm corresponds to the electronic transition of the catechol part of the chromophore. It can be seen (Fig. 1) that the absorption spectrum of **2** closely resembles that of **1** with only a slight hyperchromic effect, reflecting the minor influence of the replacement of a –OH group by a methoxy group on 3'-C. In contrast, the structural changes in **3** (substitution of the ethylenic bond by a saturated bond) cause the loss of conjugation between the quinoline part and the catechol group of the molecule which results in a significant increase of the molar absorption coefficient of the catechol group of this compound by comparison with the values obtained for the molecules **1** and **2**.

The *n*-styrylquinolines<sup>7–10,19</sup> are also characterized by a transition around 350 nm, attributed to the quinoline ring of the molecule and a distinct absorption transition around 315 nm that is characteristic of the stilbene-like chromophore. The structural modifications of the quinoline parts of compounds **1** and **2** by comparison with the 2-styrylquinolines lead to a red-shift of the latter absorption transition which is superimposed on the less intense band of the quinoline (Fig. 1). The high molar absorption coefficient values of this transition strongly suggest that the lowest excited singlet state of the molecules is of  $\pi, \pi^*$  character, as for styrylquinolines.<sup>8,19</sup> This is further confirmed by the red-shift observed in the emission spectra with increasing solvent polarity (*vide infra*).

Both the emission and excitation spectral shapes of **1** are independent of  $\lambda_{\text{ex}}$  (from 270 to 450 nm) and  $\lambda_{\text{em}}$  (from 480 to 560 nm) respectively (Fig. 2); the fact that the maximum emission is centered at 540 nm indicates that the excitation energy is largely localized in the quinoline moiety of the molecule. Furthermore, the normalized emission intensity changes observed upon excitation at different wavelengths indicate that more than one species is implicated in the absorption spectra. This was confirmed by the fluorescence excitation

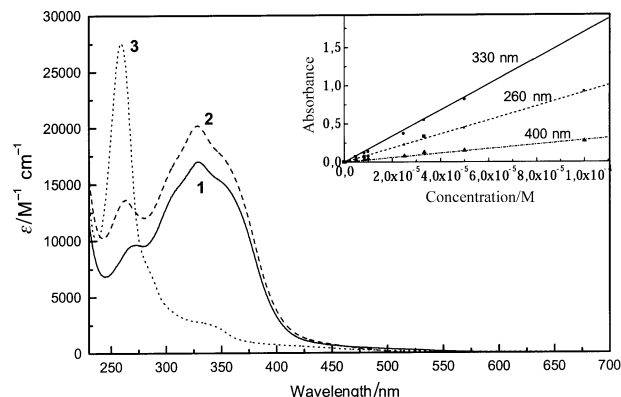


**Fig. 1** Absorption spectra of compound **1** (—) and its analogs **2** (---) and **3** (····) observed in Tris buffer pH 7.0; drug concentration  $\sim 40 \mu\text{M}$ . The inset shows the verification of the Beer-Lambert law for **1**.



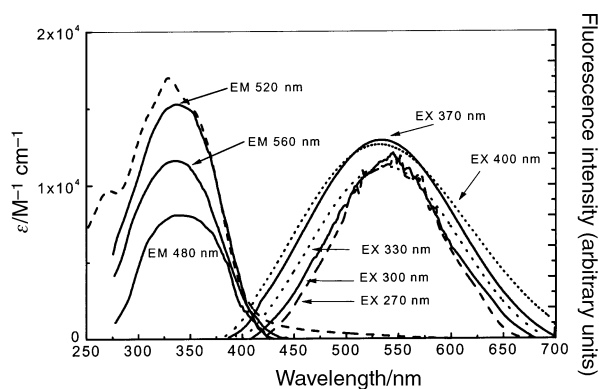


**Fig. 2** Normalized fluorescence emission (right) and corrected excitation (left) spectra of **1** (12  $\mu$ M) in Tris buffer pH 7.0, at different excitation and emission wavelengths at room temperature. The normalization is done with respect to the number of absorbed photons. The absorption spectrum (left, dashed line) is also reported for comparison.

spectrum of **1** (Fig. 2), which is less structured compared to the absorption spectrum, with only one peak around 350 nm, and could not be superimposed on the latter. Furthermore, the fluorescence decay of **1** was deconvoluted in two well-separated components, assigned to a shorter lived (30 ps) and a longer lived (230 ps) species (Table 1).

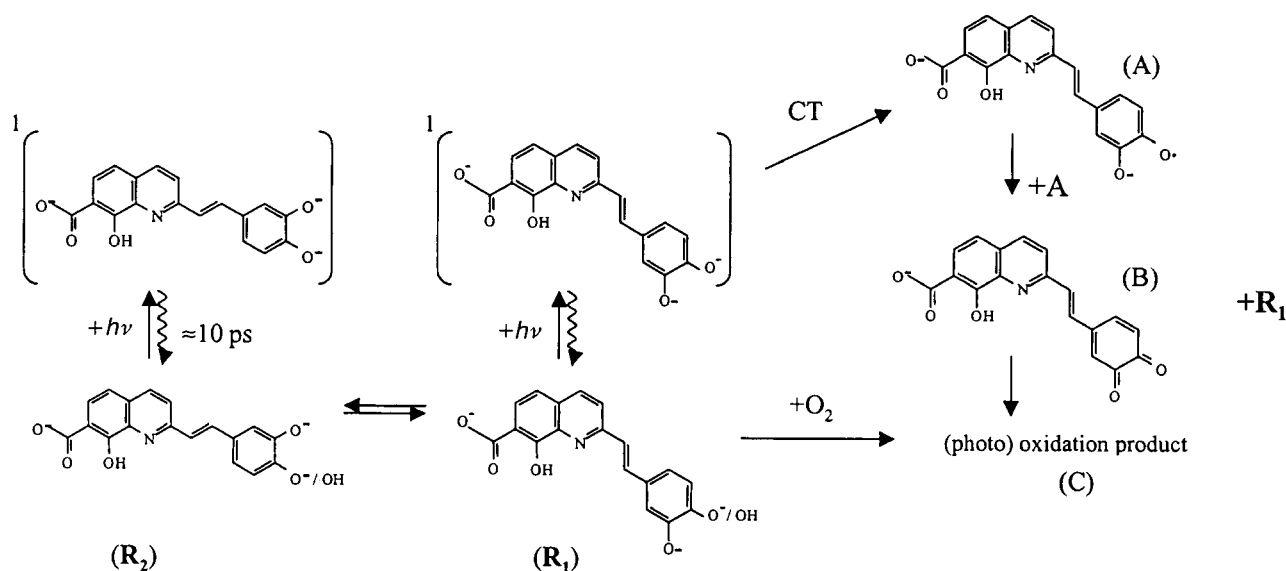
A different hypothesis can be proposed to account for these results. We have first verified that the absorbance of the drug solutions followed Beer–Lambert's law in the concentration range 5–100  $\mu$ M (Fig. 1, inset), revealing the absence of self-association of the drug in its ground state. The difference between absorption and fluorescence excitation spectra could also be explained by a  $^1\text{trans}^* \rightarrow ^1\text{cis}^*$  singlet excited state photoisomerisation of **1** as observed for styrylquinolines<sup>6,8,19,20</sup> and 2-styrylanthracene.<sup>10</sup> Such a process can be analyzed by changes in the absorption spectrum of the chromophore upon irradiation of a deoxygenated solution.<sup>8,19</sup> In our case, the absorption spectral evolution corresponds to an oxidation and not a photoisomerisation process (*vide infra*). According to the protonation state of the drug at physiological pH (*vide infra*), the existence of tautomers can also be considered on the *o*-hydroxybenzoic part of the chromophore. However, it is admitted that the neighborhood of hydroxy and carboxy substituents favors the formation of a divalent hydrogen atom link<sup>21</sup> and that the enol form prevails in solution.<sup>22</sup> Therefore, the relation of absorption, fluorescence excitation and emis-

sion properties of **1** strongly suggests the presence of at least two conformers of the molecule in the ground state. By analogy with the case of 2-styrylquinolines,<sup>7</sup> these two conformers can be assigned to two rotamers originating from the rotation of the quinoline moiety around the quasi-single bond between the quinoline and ethylenic carbon atom (Scheme 2). The relative absorption spectra of these two rotamers cannot be obtained, the stationary fluorescence emission of one of them being too weak to be detected. But, considering that the absorption spectrum of **1** corresponds to the overlapping absorption of the two rotamers in equilibrium and that the absorption maximum of one of them (**R**<sub>1</sub>) peaks at 340 nm, as revealed by its excitation spectrum, the second rotamer (**R**<sub>2</sub>) presumably has an absorption maximum at a shorter wavelength ( $\sim$ 330 nm), consistent with the lower fluorescence intensity measured for  $\lambda_{\text{exc}} < 340$  nm. This blue-shifted absorption of **R**<sub>2</sub> by comparison with **R**<sub>1</sub> indicates a larger steric repulsion between the hydrogen atoms in the **R**<sub>1</sub> rotamer. Assuming that the radiative lifetime of the two rotamers are of the same order, it may be shown, by using the relationship  $\Phi_f = \tau_f \times k_r$ , that **R**<sub>1</sub> is the component with the longer emission lifetime (230 ps) and a fluorescence quantum yield of 0.02 and that **R**<sub>2</sub> has a fluorescence lifetime of 30 ps and a quantum yield  $10 \times$  lower than that for **R**<sub>1</sub>.

### Solvent dependence of the absorption and fluorescence properties

**pH effects.** Compound **1** also undergoes pH-dependent structural changes which can be followed from the absorption spectra (Fig. 3). In acidic media, the absorption spectrum presents three main bands with peaks at 285, 340 and 415 nm. A pH increase from 2.0 to 7.0 considerably affects the spectrum. The two bands centered at 340 and 415 nm have collapsed into one major band ( $\lambda_{\text{max}} \approx 330$  nm); a blue-shift (from 285 to 270 nm) and a decrease of the maximum of the catechol transition are also observed with increasing pH. In the pH range 7.0–8.5, the spectra are quite similar with only changes in the peak intensities. Beyond pH 8.5, a gradual shift of the 330 nm maximum to 370 nm is observed, associated with an hyperchromic effect on the catechol transition (275 nm).

The drug **1** possesses various sites of protonation: at N-1 and at the oxygen atoms C-7 and C-8 of the quinoline moiety and C-3' and C-4' of the catechol part. Accurate determination of the different  $\text{pK}_a$  of the chromophore by absorption measurements alone (lack of fluorescence in acidic conditions) was impossible. However, referring to the literature, the proto-



**Scheme 2** Rotamer equilibrium between the two rotamers **R**<sub>1</sub> and **R**<sub>2</sub>, and the (photo)oxidation mechanism at pH 7.0.

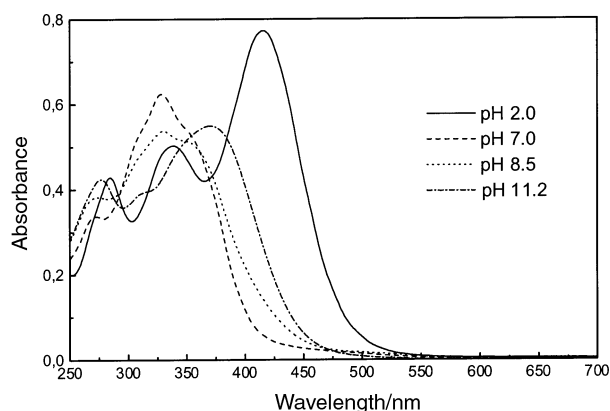


**Fig. 3** Absorption spectra of compound **1** as a function of pH. The drug concentration range is 30–40  $\mu\text{M}$ .

nation state of the molecule may be inferred from the  $\text{pK}_a$  values for each of its moieties.

The  $\text{pK}_a$  of the ground state of several *n*-styrylquinolines which possess only one protonation site on the nitrogen atom of the pyridine ring range between 4.8 and 5.8.<sup>8,23,24</sup> Furthermore, this value does not seem to be influenced by structural modifications of either the quinoline<sup>24</sup> or benzene<sup>23</sup> parts of the chromophore. Thus, similar  $\text{pK}_a$  values can be expected for the N-1 nitrogen atom of the drug. In **1**, the carboxy and hydroxy substituents lie at adjacent positions, C-7 and C-8 exactly as in *o*-hydroxybenzoic acid which has two  $\text{pK}_a$ s of 2.97 and 13 for  $\text{CO}_2\text{H}/\text{CO}_2^-$  and  $\text{OH}/\text{O}^-$  respectively.<sup>21–22</sup> Previous work<sup>25</sup> also reported two  $\text{pK}_a$ s, of 9.5 and 12.8, for the catechol group. These values should be valid for compound **3** for which the quinoline and catechol moieties are independent. In contrast, lower values should be expected for the catechol part of **1** due to the conjugation of the molecule. This hypothesis was confirmed by the results concerning the possibility of oxidation of the drug at physiological pH (*vide infra*).

The fluorescence properties of **1** as a function of pH were also investigated and the results reported in Table 1. It is known that the  $\text{pK}_a$  of the carboxy group in the singlet excited state is rather close to the  $\text{pK}_a$  value in the ground state<sup>22</sup> while both the acidity of the hydroxy group and the basicity of the ring nitrogen are enhanced in the excited state.<sup>24</sup> However, N-1 proton uptake or HO-8 proton ejection reactions, generally coupled with intramolecular electron transfer, occur on a longer time scale<sup>24</sup> than the lifetime of the singlet excited state of the drug. Consequently, it can be admitted that the singlet excited state protonation equilibrium is not attained and that the fluorescence properties of the quinoline part of the drug appear to be dependent on the protonation state of the ground state. The  $\text{pK}_a$  singlet excited state of the catechol group can reasonably be expected to be significantly lower than that of the ground state,<sup>26</sup> corresponding to an excited protonated form at pH 2.0 and a totally deprotonated form at pH  $\geq 7.0$ .

At pH 2.0 (the drug is then totally protonated), the stationary fluorescence emission of **1** is too weak to be detected. Nevertheless, the time resolved fluorescence data reveal a single exponential decay with a decay time of 20 ps (Table 1) revealing the existence of only one type of conformer. Similar results are obtained by dissolving compound **1** in borate buffer (pH 8.0). In this case, boric acid may form a complex with the *o*-hydroxybenzoic part of the molecule leading to protonation of the N-1 nitrogen atom.<sup>27</sup> This protonation results in a higher bond order of the single bond between the styryl and quinoline moieties and thus favors a conformation of the drug with a short fluorescence lifetime such as the **R**<sub>2</sub> rotamer. Beyond pH 7.0 (deprotonation of N-1 and of the

catechol part), the dynamic fluorescence data (biexponential decay, Fig. 2, Table 1) are consistent with the presence of two emissive species (no data were obtained for pH  $> 8.5$  due to significant oxidation of drug **1** under such conditions (*vide infra*)). This pH study revealed the influence of the protonation state of N-1 on the occurrence of the equilibrium between the two rotamers **R**<sub>1</sub> and **R**<sub>2</sub> of the drug.

**Polarity effects.** The absorption, excitation and fluorescence spectra of compound **1** were investigated in the non-polar solvent dioxane, and in solvents of increasing polarity, ethanol, DMSO and Tris buffer pH 7.0, in order to examine solvent effects on the photophysical properties and conformational equilibrium. Inspection of the absorption spectra shows that the catechol transition (260 nm) is practically unaffected by the solvent nature while the maximum of the main band (330–360 nm) is blue-shifted in ethanol, DMSO and water with respect to dioxane (Fig. 4(a)). In contrast, the excitation spectrum of the drug in polar solvents undergoes a small red-shift compared to the excitation spectrum measured in dioxane (Figs. 2 and 4, (b)–(d)).

The fluorescence properties of **1** are also greatly influenced by solvent properties. The fluorescence Stokes-shift is much larger ( $> 100$  nm) in polar solvents and increases with increasing solvent polarity (Fig. 4(a)). These spectral evolutions are associated with variations of the fluorescence quantum yields and lifetimes (Table 1). The fluorescence quantum yields decrease with increasing solvent polarity, except in DMSO. Similar weights of shorter (a few tens of picoseconds) and longer lived (a few hundreds of picoseconds) components are observed in ethanol and water while in dioxane fluorescence occurs only from two longer lived components. While DMSO is a protic solvent, the longer lived decay components are similar to those for dioxane.

The photophysical properties of **1** in dioxane, DMSO and ethanol by comparison with the results obtained in water indicate that the conformational equilibrium of the drug changes with solvent properties. Referring to the absorption and excitation spectra, it appears that the protic character of the solvent favors the occurrence of an equilibrium distribution of conformers of the drug. Considering the fluorescence lifetimes, the shorter lived component observed in ethanol and DMSO (20–50 ps) can be attributed to the **R**<sub>2</sub> rotamer and the hundreds of picoseconds one (650–780 ps) to the **R**<sub>1</sub> rotamer, already described in the case of water. On a longer time scale,

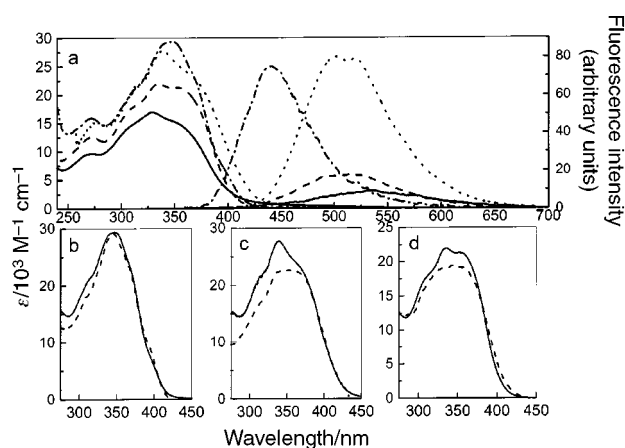


**Fig. 4** (a) Absorption spectra (left) and fluorescence spectra (right) of compound **1** in dioxane, ethanol, DMSO and Tris buffer pH 7.0. The drug concentration is 1  $\mu\text{M}$  in dioxane (---) and DMSO (-----), 5  $\mu\text{M}$  in ethanol (---) and 12  $\mu\text{M}$  in aqueous solution (—). The fluorescence spectra are normalized to the same absorbance at the excitation wavelength (360 nm). (b), (c), (d), Comparison of the absorption (—) and excitation fluorescence (---) spectra of **1**, in respectively, dioxane ( $\lambda_{\text{em}} = 440$  nm), DMSO ( $\lambda_{\text{em}} = 520$  nm) and ethanol ( $\lambda_{\text{em}} = 540$  nm).

the fluorescence emission analysis in DMSO and ethanol is more complex than in water, an additional component in the nanosecond time range is observed. Due to the superposition of the fluorescence excitation spectra at various emission wavelengths, the existence of a new conformer in the fundamental state can be reasonably excluded both in ethanol and DMSO. Therefore, the nanosecond fluorescence component probably arises from a singlet excited state reaction, the nature of which falls beyond the scope of the present paper. The excitation spectrum of **1** in dioxane is roughly the image of its absorption spectrum with a maximum at 350 nm (Fig. 4(b)) and the absence of the tens of picoseconds fluorescence lifetime suggests the presence of only the  $R_1$  rotamer in this solvent. The nanosecond fluorescence component can be explained in the same way as in ethanol and DMSO. This solvent polarity study reveals that even though the  $R_2$  conformer has a larger steric repulsion than the conformer  $R_1$ , its formation is favored in protic solvents, a result already observed for 2-styrylquinoline.<sup>7</sup>

### Spectral evidence for the formation of an oxidized form in aqueous solution

The absorption spectra of **1** in Tris buffer pH 7.0 under atmospheric pressure was found to evolve with time after preparation while kept in the dark (Fig. 5). It is seen that the lower-energy absorption band centered at 330 nm decreases with time while the second band increases and is blue-shifted from 270 to 260 nm and a new transition appears at 440 nm. Moreover, the presence of an isosbestic point at 395 nm strongly suggests the formation of a new species in the ground state.

The following facts suggest that **1** can be oxidized: (i) no spectral evolution was observed in anaerobic conditions or at pH 2.0 (even in the presence of oxygen) corresponding to a totally protonated form of the drug (see above), (ii) the absorption spectrum evolution increased on the one hand with increasing pH (for pH > 7.0) in correlation with deprotonation of the catechol group of the molecule (*vide supra*) and on the other hand with oxygen pressure (from atmospheric pressure to 1 atm of  $O_2$ ) and (iii) the spectral evolution is less pronounced with compound **2** which possesses only one OH group on its benzene part and is absent for **3** which is still protonated on its catechol part in the pH range 7.0–9 (*vide supra*). The oxidation depends on how long the solutions are exposed to air and on the protonation state of the drug

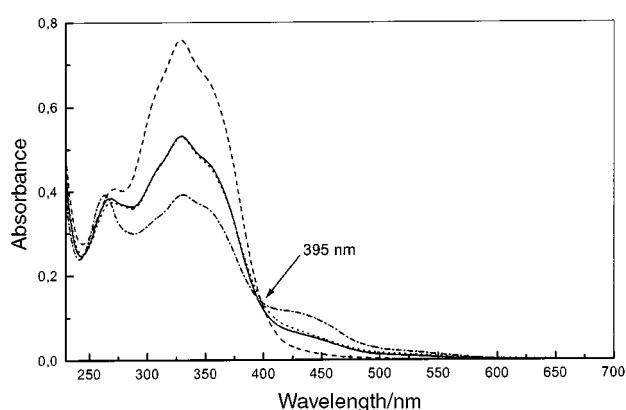


**Fig. 5** Absorption spectral changes of **1** solutions (45  $\mu$ M) in deaerated Tris buffer, pH 7.0, as a function of fluence upon irradiation with a xenon lamp ( $\lambda > 325$  nm) or with a nanosecond laser source: (---) before irradiation, (—)  $6 \times 10^4$  J m<sup>-2</sup>, (-·-·-)  $1.5 \times 10^5$  J m<sup>-2</sup>. The spectrum obtained after 2 h (····) in the absence of irradiation but under aerated conditions is superimposed on that obtained upon irradiation with a fluence of  $6 \times 10^4$  J m<sup>-2</sup>.

(for pH  $\geq 10$ , oxidation was initiated as soon as the drug was diluted into the buffer).

Upon steady state irradiation of deoxygenated solutions of **1**, a similar evolution of the absorption spectrum is observed (Fig. 5) as in the presence of oxygen, but it takes place much faster. These results indicate that, upon light activation, photooxidation of the drug also occurs.

A likely mechanism proposed for the reaction of oxygen with a catechol<sup>17</sup> is the formation of a semiquinone radical by one-electron oxidation followed by dismutation of this radical giving rise to an orthoquinone species which typically absorbs at  $\lambda \approx 420$  nm. Such an oxidation pathway can account for the spectral evolution observed with **1** in the presence of oxygen. It must be noted that the orthoquinone formed is also unstable; after resting for one day in the dark, the spectrum of the oxidized drug has undergone further changes.

Since similar spectral evolutions are observed under photolysis of **1** in anaerobic conditions and in the presence of oxygen (Fig. 5), we can predict that the semiquinone radical is also the main intermediate upon light activation of the drug. To verify this hypothesis and to investigate the photooxidation mechanism of **1**, time resolved absorption spectroscopy experiments have been performed.

### Nanosecond and subpicosecond laser photolysis

Fig. 6 shows the transient spectra obtained from 355 nm laser excitation of **1** in  $N_2O$ ,  $N_2$  or  $O_2$  saturated Tris buffer solution at pH 7.0, recorded at different delay times after the end of the pulse. The difference spectrum recorded at the end of the laser pulse is characterized by a positive broad band with a maximum at 430 nm and a negative band due to ground state depletion around 330 nm. The dependence of the signal at 430 nm on the laser energy is linear up to an incident fluence of 40 mJ cm<sup>-2</sup>, as expected for a monophotonic process. By increasing the energy of the excitation pulse, the transient absorbance greatly increased and was followed by a rapid decay (only a few nanoseconds) of the signal, which is consistent with the occurrence of an additional photophysical process. Thus, the excitation of compound **1** was performed under energy conditions such that this second transient was not significantly formed.

The transient spectrum measured at the end of the laser pulse in  $N_2$  is coincident both in shape and intensity with those obtained in the presence of efficient hydrated electron scavengers ( $N_2O$  and  $O_2$ ), a result which leads to the conclusion that photoionization is not involved in the laser photolysis

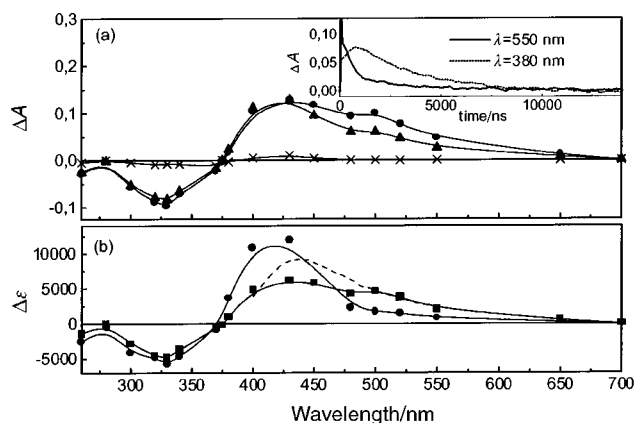
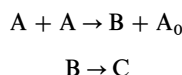


**Fig. 6** (a) Transient difference absorption spectra measured on 355 nm photolysis of compound **1** (40  $\mu$ M) in 20 mM Tris buffer pH 7.0, under  $N_2O$  saturation: delay time (●) 10 ns, (▲) 400 ns, (\*) 10  $\mu$ s. Inset: Time profile observed at different characteristic wavelengths. (b) Spectra of (■) A and (●) B species according to the analytical model. The dashed line spectrum is adjusted to the absorbance spectrum obtained at 400 ps delay by subpicosecond laser photolysis.



sis of the drug. Furthermore, typical triplet quenchers such as oxygen (under 1 atm), piperylene (0.1 M) or 1-naphthalenemethanol ( $10^{-3}$  M) had no effect on the transient absorption spectrum, revealing that the corresponding species is not an excited triplet state. In agreement with this conclusion, the spectral absorbance evolution is characterized by the formation, on the nanosecond time scale, of a new transient (build-up of the absorbance for wavelengths between 400 and 430 nm) (Fig. 6, inset), followed by a decrease of the transient absorbance over all the spectral range on the microsecond time scale.

The absorbance changes (Fig. 6(a)) can be analyzed at each wavelength on the basis of two consecutive reactions corresponding, respectively, to second order and first order kinetics according to the following scheme:



where A corresponds to the transient species observed at the end of the laser pulse,  $A_0$  to the drug in its fundamental state, B to the product of dismutation and C to the species generated by the disappearance of B. In this kinetic scheme, we suggest that A corresponds to a radical species. In view of the structure of **1**, two mechanisms can be proposed: a photodecarboxylation involving the formation of a carbanion on the quinoline part,<sup>28–30</sup> or the formation of a semiquinone radical from the deprotonated catechol group of the chromophore. To check a pathway involving decarboxylation, laser photolysis experiments were carried out with drug **1** as a function of pH (pH 2.0, 7.0, 8, 8.5) and with the compounds **2** and **3** at pH 7.0 (using energy laser conditions corresponding to a monophotonic process). The results reveal that (i) no transient signal was observed for the fully protonated form of **1** (pH 2.0) nor for compound **3** and (ii) similar transient absorptions were detected for compounds **1** and **2** at  $\text{pH} \geq 7.0$  (corresponding to partial deprotonation of the catechol part of the chromophores). A photodecarboxylation process should be independent of both these pH conditions and structural modifications between the different compounds studied and thus such a process can reasonably be excluded. Therefore the transient absorption spectrum measured at the end of the nanosecond laser pulse can be attributed to the semiquinone radical that originates from a charge transfer reaction occurring on a time scale faster than nanoseconds (*vide infra*). This was confirmed by experiments performed in the presence of various amounts of ascorbic acid, a quencher of semiquinone radicals.<sup>25</sup> An efficient radical quenching with a rate constant of  $2.5 \times 10^7 \text{ M}^{-1} \text{ s}^{-1}$  was observed.

The semiquinone radical was found to evolve by a dismutation reaction ( $k = 3 \times 10^{10} \text{ M}^{-1} \text{ s}^{-1}$ ) leading simultaneously to the formation of the ground state of the drug ( $A_0$ ) and of a species (B) absorbing predominantly at 420 nm (Fig. 6(a)), assigned to an orthoquinone. The analytical model allows the determination of the absorption spectra of both semiquinone and orthoquinone (Fig. 6(b)). The orthoquinone first formed is unstable and decays ( $k = 4.5 \pm 0.3 \times 10^5 \text{ s}^{-1}$ ) to give the more stable photoproduct (C) already observed by steady state absorption and not yet identified (Fig. 5).

As stated above, the hypothesis of a semiquinone radical formation requires a charge transfer reaction as the precursor step, a process which probably occurs on the picosecond time scale. This was confirmed by experiments performed using subpicosecond laser excitation.

The transient absorption spectrum obtained at 1.5 ps by 320 nm subpicosecond laser photolysis of compound **1** is characterized by one main band, centered at 460 nm. (Fig. 7). The transient absorbance develops out within the laser pulse duration, as illustrated in Fig. 8(a). Since both  $R_1$  and  $R_2$  rotamers can be excited at 320 nm, the transient spectrum is likely

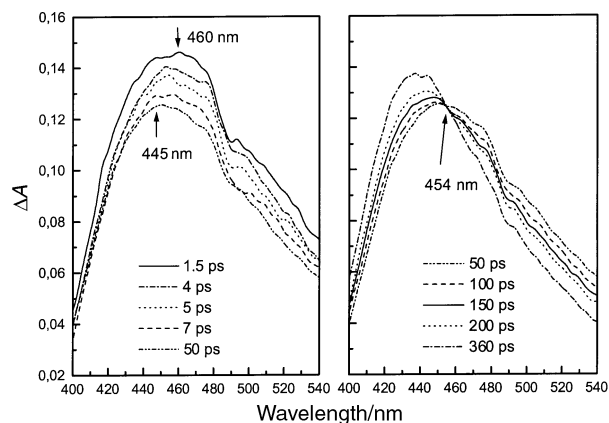


Fig. 7 Transient difference absorption spectra measured on 320 nm photolysis of compound **1** ( $[1] = 40 \mu\text{M}$ ) in 20 mM Tris buffer pH 7.0 as a function of time.

to be due to the sum of the excited singlet state  $S_1$  absorption of both rotamers. The kinetics of this differential absorption reveals a fast component of  $8 \text{ ps} \pm 2 \text{ ps}$  (Fig. 8(b)). Accordingly, a spectral evolution was also identified which can be quantitatively represented by the first momentum of the absorption spectrum defined by:

$$\bar{\nu} = \frac{\int \nu A(\nu) d\nu}{\int A(\nu) d\nu}$$

where  $\nu$  is the wavenumber and  $A$  the measured transient absorption. A spectral displacement ( $\Delta\nu \approx 2 \times 10^{13} \text{ s}^{-1}$ ) ( $\Delta\lambda \approx 13 \text{ nm}$ ) was thus found at the end of the fast process (Fig. 8(c)).

The time constant of this process closely matches the fast decay of the fluorescence intensity (30 ps) (taking into account the experimental accuracy in the time resolved fluorescence measurements) indicating that it could correspond to  $S_1$  decay of the  $R_2$  rotamer. From these assignments, the transient absorption spectrum measured at 50 ps ( $\lambda_{\text{max}} \approx 445 \text{ nm}$ ) can be attributed to the  $S_1$  absorption of the  $R_1$  rotamer which has not started to evolve because of its much longer fluorescence lifetime (Table 1).

Clearly (Fig. 7, 8(c)) at times later than 50 ps, the decay of the band centered at 445 nm is accompanied by the rise of a band centered at 430 nm with the same time constant of 200 ps. The existence of an isosbestic point at 454 nm indicates that the  $R_1$  rotamer in its singlet excited state interconverts into a new transient species. One notes a close similarity between the spectra obtained at 360 ps delay in subpicosecond

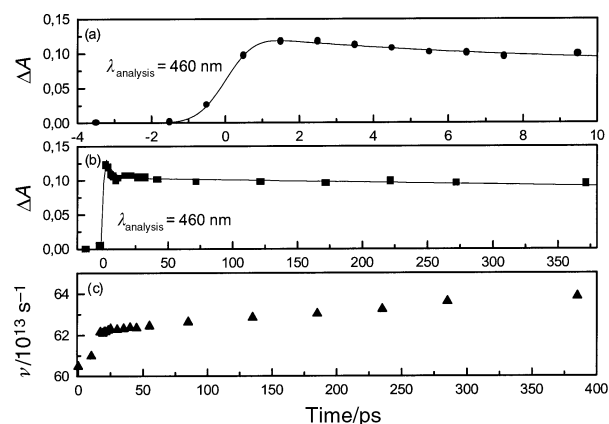


Fig. 8 (a) Rise of the difference absorbance of **1** in aqueous solution at pH 7.0 upon 320 nm laser excitation. (b) Decay of the difference absorbance of the same solution. (c) Plot of the first momentum of the absorption spectrum against the delay time.



measurements and at the end of the nanosecond laser excitation (Fig. 6(b)), meaning that the semiquinone radical is already formed at 400 ps. It may be noted that the maximum of the nanosecond spectrum is less intense than that of the picosecond one (Fig. 6(b)) due to the fact that the dismutation reaction has begun to occur on the subnanosecond time scale.

The semiquinone radical formation requires an intramolecular electron transfer between the catechol and quinoline parts of the drug which may occur consecutively to energy redistribution in the excited states as reported for such complex molecules.<sup>29,30</sup> This electron transfer process can be mediated by singlet–triplet intersystem crossing. However, a common feature for a number of stilbene<sup>9</sup> and styryl derivatives<sup>6,31</sup> is the very low intersystem crossing quantum yield. Thus,  $S_1$  is therefore more likely to be the reactive excited state.

## Conclusion

In this study, it has been shown that compound **1** is present in solution as a mixture of two stable rotamers with different photophysical and photochemical properties. The equilibrium between the conformers is strongly pH and solvent dependent. In acidic medium, only the  $R_2$  rotamer (Scheme 2) is present while in aprotic solvents (dioxane) only the  $R_1$  rotamer exists. The structural differences between the two conformers are mainly reflected in their singlet excited state lifetimes. The  $R_2$  rotamer fluoresces in only a few picoseconds while the  $R_1$  rotamer has a longer excited state lifetime, ranging from a few hundreds of picoseconds to nanoseconds, depending on the solvent characteristics. This study reveals that the physicochemical properties of **1** are clearly related to its spectroscopic properties which are quite sensitive to its environment.

It was also shown that the  $R_1$  rotamer can undergo oxidation or photooxidation involving a semiquinone radical as the key intermediate. Upon photolysis, this radical is formed from the excited singlet state which deactivates through intramolecular electron transfer from the catechol to the quinoline moieties. The electronic conjugation of the molecule is the key condition for the occurrence of such a (photo)oxidation process. The possible occurrence of such oxidation at physiological pH can be a limiting factor for its biological activity. This finding has prompted the synthesis of novel drugs for which oxidation is precluded while the cellular activity is retained.

## References

- 1 D. J. Hazuda, P. Felock, M. Witmer, A. Wolfe, K. Stillmock, J. A. Grobler, A. Espeseth, L. Gabryelski, W. Schleif, C. Blau and M. D. Miller, *Science*, 2000, **287**, 646.
- 2 K. Mekouar, J. F. Mouscadet, D. Desmaële, F. Subra, H. Leh, D. Savouré, C. Auclair and J. d'Angelo, *J. Med. Chem.*, 1998, **41**, 2846.
- 3 F. Zouhiri, J. F. Mouscadet, K. Mekouar, D. Desmaële, D. Savouré, H. Leh, F. Subra, M. Le Bret, C. Auclair and J. d'Angelo, *J. Med. Chem.*, 2000, **43**, 1533.
- 4 M. Ouali, C. Laboulais, H. Leh, D. Gill, D. Desmaële, K. Mekouar, F. Zouhiri, J. d'Angelo, C. Auclair, J. F. Mouscadet and M. Le Bret, *J. Med. Chem.*, 2000, **43**, 1949.
- 5 D. H. Waldeck, *Chem. Rev.*, 1991, **91**, 415.
- 6 U. Mazzucato and F. Momicchioli, *Chem. Rev.*, 1991, **91**, 1679.
- 7 S. C. Shim, D. W. Kim and M. S. Kim, *J. Photochem. Photobiol. A*, 1991, **56**, 227.
- 8 G. Galianzo, G. Gennari and P. Bortolus, *J. Photochem.*, 1983, **23**, 149.
- 9 G. Gennari, P. Bortolus and G. Galianzo, *J. Mol. Struct.*, 1991, **249**, 189.
- 10 A. Spalletti and G. Bartocci, *Phys. Chem. Chem. Phys.*, 1999, **1**, 5623.
- 11 S. R. Meech and D. Phillips, *J. Photochem.*, 1983, **23**, 193.
- 12 Ph. Wahl, in *New Techniques in Biophysics and Cell Biology*, ed. M. Pain and B. Smith, John Wiley & Sons, Chichester, 1975, vol. 2, p. 233.
- 13 D. V. O'Connor and D. Philips, in *Time-correlated Single Photon Counting*, Academic Press, London, 1984.
- 14 J.-C. Brochon, *Methods Enzymol.*, 1994, **240**, 262.
- 15 A. K. Liversey and J.-C. Brochon, *Biophys. J.*, 1987, **52**, 693.
- 16 M. Enescu, M. P. Fontaine-Aupart, B. Soep and F. Tfibel, *J. Phys. Chem. B*, 1998, **102**, 3631.
- 17 R. C. Bensasson, C. Land and R. G. Truscott, in *Excited States and Free Radicals in Biology and Medicine*, Oxford University Press, New York, 1993, pp. 80–82 and 236–239.
- 18 M. P. Fontaine-Aupart, E. Renault, C. Videlot, F. Tfibel, R. Pansu, M. Charlier and P. Pernot, *Photochem. Photobiol.*, 1999, **70**, 829.
- 19 G. Gennari, G. Galianzo and P. Bortolus, *J. Photochem.*, 1986, **35**, 177.
- 20 R. Zamboni, M. Belley, E. Champion, L. Charette, R. DeHaven, R. Frenette, J. Y. Gauthier, T. R. Jones, S. Leger, P. Masson, C. S. McFarlane, K. Metters, S. S. Pong, H. Pierachuta, J. Rokach, M. Thérien, H. W. R. Williams and R. N. Young, *J. Med. Chem.*, 1992, **35**, 3832.
- 21 *Handbook of Chemistry and Physics*, The Chemical Rubber Company, Boca Raton, FL, p. D86.
- 22 G. S. Denisov, N. S. Golubev, V. M. Schreiber, Sh. S. Shajakhmedov and A. V. Shurukhina, *J. Mol. Struct.*, 1997, **437**, 153.
- 23 S. W. Wang and T. I. Ho, *Chem. Phys. Lett.*, 1997, **268**, 434.
- 24 E. Bardez, A. Chatelain, B. Larrey and B. Valeur, *J. Phys. Chem.*, 1994, **98**, 2357.
- 25 Z. B. Alfassi and R. H. Shuler, *J. Phys. Chem.*, 1985, **89**, 3359.
- 26 C. A. Parker, in *Photoluminescence of Solutions*, Elsevier, Amsterdam, 1968, ch. 4.
- 27 *Traite de Chimie minérale de Pascal*, volume of borine, Masson, 1933, pp. 220–222 and 304–308.
- 28 F. Bosca and M. A. Miranda, *Photochem. Photobiol.*, 1999, **70**, 653.
- 29 S. Encinas, M. A. Miranda, G. Marconi and S. Monti, *Photochem. Photobiol.*, 1998, **68**, 633.
- 30 S. Sortino and J. C. Scaiano, *Photochem. Photobiol.*, 1999, **69**, 167.
- 31 G. G. Aloisi, F. Elisel and L. Latterini, *J. Chem. Soc., Faraday Trans.*, 1992, **88**, 2139.